MNRAS **000**, 1–6 (2017) Preprint 2 February 2017 Compiled using MNRAS LATEX style file v3.0

Direct evidence for Lyα depletion in the protocluster core

Rhythm Shimakawa,[1,2]⋆ Tadayuki Kodama,[1,2]† Masao Hayashi,[2] Ichi Tanaka,[3] Yuichi Matsuda,[1,2] Nobunari Kashikawa,[1,2] Takatoshi Shibuya,[4] Ken-ichi Tadaki,[5] Yusei Koyama,[1,3] Tomoko L. Suzuki[1,2] and Moegi Yamamoto[1]

[1] *Department of Astronomical Science, SOKENDAI, Osawa, Mitaka, Tokyo 181-8588, Japan*
[2] *National Astronomical Observatory of Japan, Osawa, Mitaka, Tokyo 181-8588, Japan*
[3] *Subaru Telescope, National Astronomical Observatory of Japan, 650 North A'ohoku Place, Hilo, HI 96720, USA*
[4] *Institute for Cosmic Ray Research, The University of Tokyo, 5-1-5 Kashiwanoha, Kashiwa, Chiba 277-8582, Japan*
[5] *Max-Planck-Institut für Extraterrestrische Physik, Giessenbachstrasse, D-85748 Garching Germany*

arXiv:1702.00100v1 [astro-ph.GA] 1 Feb 2017

Accepted 2017 January 31. Received 2017 January 18; in original form 2016 December 22

ABSTRACT

We have carried out a panoramic Lyα narrowband imaging with Suprime-Cam on Subaru towards the known protocluster USS1558–003 at $z = 2.53$. Our previous narrowband imaging at near-infrared has identified multiple dense groups of Hα emitters (HAEs) within the protocluster. We have now identified the large-scale structures across a ∼50 comoving Mpc scale traced by Lyα emitters (LAEs) in which the protocluster traced by the HAEs is embedded. On a smaller scale, however, there are remarkably few LAEs in the regions of HAE overdensities. Moreover, the stacking analyses of the images show that HAEs in higher-density regions show systematically lower escape fractions of Lyα photons than those of HAEs in lower-density regions. These phenomena may be driven by the extra depletion of Lyα emission lines along our line of sight by more intervening cold circumgalactic/intergalactic medium and/or dust existing in the dense core. We also caution that all the past high-z protocluster surveys using LAEs as the tracers would have largely missed galaxies in the very dense cores of the protoclusters where we would expect to see any early environmental effects.

Key words: galaxies: formation – galaxies: evolution – galaxies: high-redshift

1 INTRODUCTION

High-z galaxy protoclusters (Sunyaev & Zeldovich 1972) are ideal test beds where we can understand how cluster galaxies form and grow during the course of cosmic mass-assembly history and the build-up of large-scale structures (LSSs) in the Universe (White & Frenk 1991; Cole et al. 2000). They directly inform us of what is occurring in the early phase of cluster formation and galaxy formation therein, which then tells us what the physical mechanisms are that lead to the galaxy diversity depending on the environment seen in the local Universe (Dressler 1980; Cappellari et al. 2011).

The observational limitation due to the Earth's atmosphere has created a gulf between high-z galaxy surveys at $z < 2.6$ and those at $z > 2.6$. At redshifts greater than 2.6, bright H$\alpha\lambda$6565 emission line is no longer observable from ground-based telescopes, and the Ly$\alpha\lambda$1216 line is the most commonly used spectral feature of star-forming galaxies that can be captured by optical instruments. This technique has been widely used to identify galaxies at high redshifts both in the general fields and in overdense regions such as protoclusters (Ouchi et al. 2003; Venemans et al. 2007). However, we know that only a small fraction of star-forming galaxies show detectable Lyα emission lines (Hayes et al. 2010; Matthee et al. 2016; Hathi et al. 2016). Furthermore, the environmental dependence of Lyα emitters (LAEs) has largely been unexplored yet. Therefore, understanding the dependence of physical properties and the selection effects of LAEs across various environments is strongly desired.

In this respect, the dual emitter surveys of HAEs and LAEs for the known protoclusters at $z = 2.1$–2.6 can play a key role in testing the Lyα selection effect for high-z protocluster search. This *letter* studies Lyα emissivities of Hα-emitting galaxies in a known dense protocluster, USS 1558–003 at $z = 2.53$ ($\alpha_{\rm J2000} = 16^{\rm h}01^{\rm m}17^{\rm s}$ $\delta_{\rm J2000} = -00^{\rm d}28^{\rm m}47^{\rm s}$, hereafter USS 1558) discovered by Kajisawa et al. (2006); Kodama et al. (2007); Hayashi et al. (2012) with MOIRCS on the Subaru telescope. Our recent deep Hα narrowband survey of this region succeeded in detecting more protoclus-

⋆ rhythm.shimakawa@nao.ac.jp
† t.kodama@nao.ac.jp

© 2017 The Authors

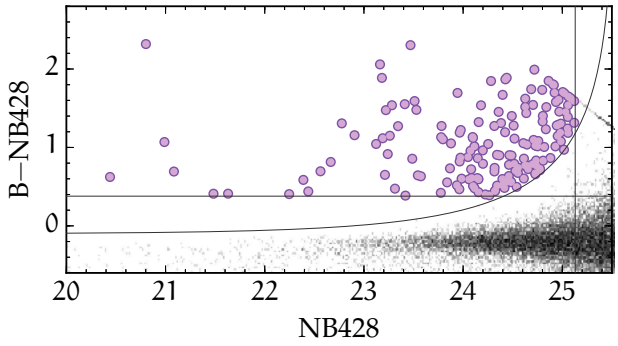

Figure 1. The colour–magnitude diagram. The black shows the NB-detected sources. The purple circles indicate narrow-band emitters that meet our criteria, namely (1) the line EW is greater than > 15 Å in the rest-frame (the horizontal line), (2) line flux excess is larger than 3σ (the black curve), and the detection at NB428 is more than 5σ levels (the vertical line).

ter members amounting to 100 HAEs in total (Hayashi et al. 2016), allowing us to characterise sub-structures such as clumps associated to USS 1558. Given such a unique laboratory of overdense environment at $z = 2.5$, we have manufactured a dedicated narrowband filter for this specific target and installed it on the Suprime-Cam so that we can also target LAEs associated with this region. Also, the wider field of view of Suprime-Cam (32'×27') compared to MOIRCS (7'×4') enables us to map LSSs in and around USS 1558.

We assume the cosmological parameters of $\Omega_M = 0.3$, $\Omega_\Lambda = 0.7$ and $h = 0.7$ and employ a Chabrier (2003) stellar initial mass function, and the AB magnitude system (Oke & Gunn 1983) are used throughout the *Letter*. Galactic extinctions at NB428 and B-band are assumed to be 0.55 and 0.57 mag, respectively (Schlegel et al. 1998; Fitzpatrick 1999; Schlafly & Finkbeiner 2011)[1].

2 OBSERVATION AND DATA ANALYSES

We performed Lyα line imaging of USS 1558 at $z = 2.53$ with the Subaru Prime Focus Camera (Suprime-Cam; Miyazaki et al. 2002) on the Subaru telescope. We used the custom-made narrowband filter NB428 that has the central wavelength of 4297 Å and FWHM of 84 Å. This is designed so that the filter FWHM neatly captures the Lyα lines at $z = 2.53 \pm 0.03$ (emission or absorption) from HAEs at $z = 2.52 \pm 0.02$ associated with the USS 1558 protocluster selected by the narrowband filter, NB2315, installed on MOIRCS/Subaru (see Shimakawa et al. 2016)[2]. The combined analysis of a resonant Lyα line by NB428 and a non-resonant Hα line by NB2315 enables us to make the first systematic comparison of spatial distributions between LAEs and HAEs, and to investigate the environmental dependence of the Lyα photon escape fractions within the protocluster.

The observation was executed on June 10 in 2015 under a photometric condition but with a relatively bad seeing (FWHM=0.8–1.4 arcsec). The science frames with seeing sizes worse than 1.3 arcsec were trashed and we used 19 frames of 700 sec exposures each, amounting to 3.7 hrs of net integration time in total. The data were reduced in exactly the same way as in Shimakawa et al. (2016) based on a data reduction package for the Suprime-Cam, SDFRED (ver.2; Yagi et al. 2002; Ouchi et al. 2004). The pipeline includes the standard procedures. The sky subtraction was conducted with the mesh size of 13 arcsec. We additionally implemented a cosmic ray reduction using the algorithm, L.A.Cosmic (van Dokkum et al. 2011). The final combined image has a seeing size of FWHM = 1.24 arcsec, and the limiting magnitude of 25.13 mag at 5 sigma with 2.5 arcsec aperture diameter reckoning with the galactic extinction.

Combining the reduced NB428 data with the existing counterpart B-band image ($B_{5\sigma} = 25.72$ mag with 2.5 arcsec aperture diameter) provided by Hayashi et al. (2016), we select LAE candidates in the same manner as in Shimakawa et al. (2016). Here, the seeing FWHM of B-band is tuned to that of the NB428 image. The object photometry is performed by SExtractor (ver.2.19.5; Bertin & Arnouts 1996). Photometric measurements are done in the double image mode using the narrowband image for source detections, and we employed aperture photometries with 2.5 arcsec diameter. This work imposes the selection criteria as follows; (1) narrowband flux excess is greater than 3σ with respect to the photometric error, (2) Lyα equivalent width is higher than $\mathrm{EW}_{\mathrm{Ly}\alpha} = 15$ Å in the rest frame, and (3) $NB_{5\sigma} < 25.13$ mag. The correction factor of the colour term (i.e. zero point of B−NB) is assumed to be −0.1, which is tailored to that in our past study of another field using the same NB428 filter (Shimakawa et al. 2016). 2σ limiting magnitude are assumed for the sources with B-band detection levels lower than 2σ.

As a result, in total 162 objects satisfied our selection criteria (Fig. 1). This *Letter* employs these samples as LAE candidates at $z = 2.5$. However, it is noted that a considerable number of foreground contaminations such as [OII]$\lambda\lambda$3727, 3730, CIV$\lambda\lambda$1548, 1551 would be contained even though we are targeting the region that hosts the known protocluster (c.f. $\sim$ 60 % in the random field according to Sobral et al. 2016). The currently available photometric data that cover the entire field are only B, r, and z-band photometries with Suprime-Cam, which are not sufficient to cleanly decontaminate our LAE samples. This caution should be kept in mind when our LAE samples are discussed.

3 RESULTS

Figure 2a shows the spatial distribution of the LAE candidates over the entire field of Suprime-Cam. The protocluster cores traced by the HAEs with MOIRCS in our previous studies (Hayashi et al. 2012, 2016) are embedded in the much larger-scale structures traced by LAEs. Hayashi et al. (2016) have identified 100 HAEs based on the combined

[1] http://irsa.ipac.caltech.edu/applications/DUST/

[2] The bandpass of NB428 for Lyα does not perfectly match to that of NB2315 for Hα. This leads to 10 % Lyα flux loss on average for HAEs which is considered in our stacking analyses (§4). Also, the NB2315 bandpass shifts blueward towards the edge of MORICS field of view, however, this effect can be negligible for our HAE samples according to the past follow-up spectroscopy (Shimakawa et al. 2014). Furthermore, NB428 covers up to higher redshifts for Lyα by $\gtrsim$ 1500 km s^{-1} with respect to that of NB2315 for Hα, and thus a possible redward velocity offset of Lyα relative to Hα (Shapley et al. 2003) would be negligible.

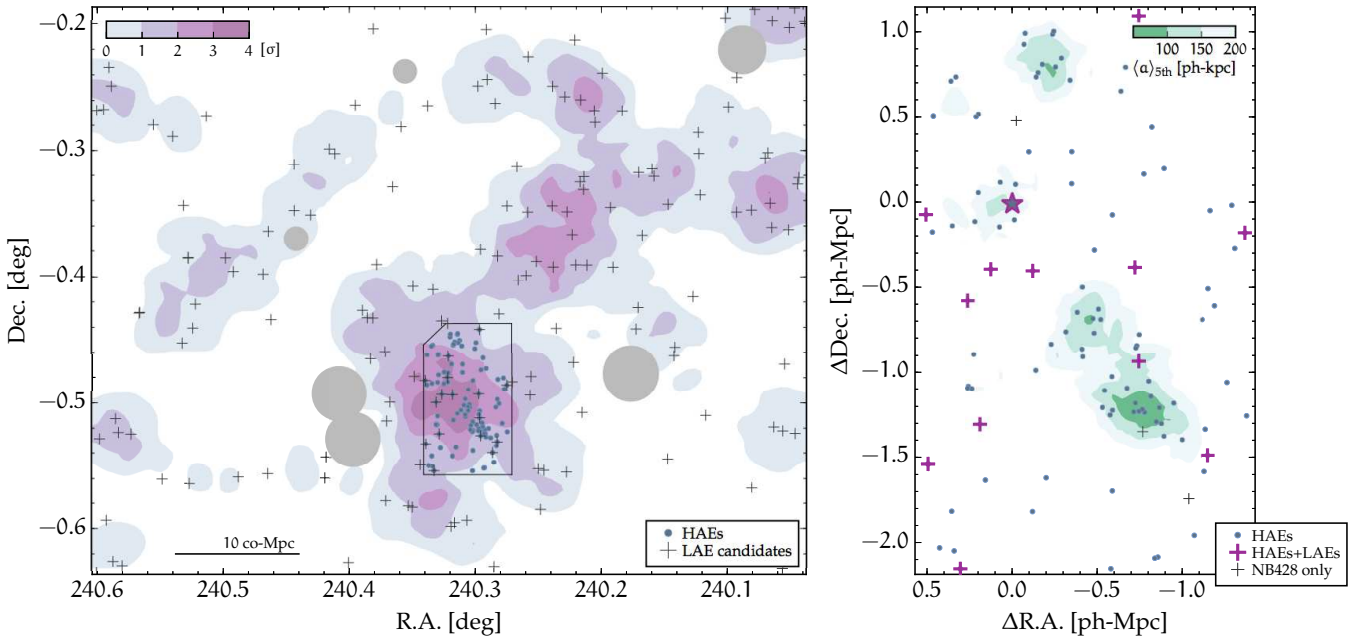

Figure 2. The 2-D maps of USS 1558 protocluster with Suprime-Cam (a: left) and with MOIRCS (b: right). (a) The black crosses represent the LAE candidates, and the blue circles indicate the HAEs identified by Hayashi et al. (2016). The filled contours indicate the significance of LAE overdensities (0–σ, σ–2σ, 2σ–3σ, and 3σ–4σ), which are smoothed by the Gaussian kernel of $\sigma = 1$ degree. The region enclosed by the black lines corresponds to the survey field of MOIRCS for HAEs. (b) The symbols are the same as shown in the left panel, but the purple crosses show the dual Hα and Lyα emitters. The star symbol indicates the RG. The filled contours shows the mean distance of, 200–150, 150–100, and <100 ph-kpc (physical kpc), smoothed by the Gaussian kernel of $\sigma = 0.5$ arcmin.

technique of the narrowband selection and two colour–colour diagrams (r'JKs and r'H_{F160W}Ks). These samples are limited to the star-formation rates (SFRs) of >2.2 $M_\odot$/yr without dust correction. 41 among those HAEs have been spectroscopically confirmed by Shimakawa et al. (2014, 2015). Also from those spectroscopic analyses, we reckon that the contamination in the rest of our unconfirmed HAEs is less than 10 %. This protocluster core contains four very dense groups of HAEs; one in the immediate vicinity of the radio galaxy (RG), two toward the southwest (the further one is the densest), and one to the north of RG (Fig. 2b). Within the MOIRCS survey field, we identify significant Lyα emission lines for nine HAEs including the RG, which meet our LAE criteria. We also find four more objects which have both Lyα and Hα detections in the two narrowbands, which were deselected from our original HAE samples in Hayashi et al. (2016) by their colour–colour criteria. Including those, 104 HAEs are now identified in total as protocluster members, and 13 out of those are also classified as LAEs. On the other hand, three LAE candidates show no Hα emission line in our previous narrowband imaging at NIR. Some of these are likely to be foreground contaminations (other emitters than Lyα) and the rest would be too faint HAEs.

LAE density map shows a 4σ excess peak just around the mainbody of the protocluster USS 1558 traced by HAEs. The notable LSS or a gigantic filament extends toward northwest. A follow-up spectroscopy is needed to confirm the structures since our LAE samples would contain foreground other line contaminations. Surprisingly, however, on a much smaller scale (∼300 physical kpc (ph-kpc)), HAEs with Lyα line detections are distributed as if they are trying to avoid the overdense groups of HAEs (Fig. 2b). It is remarkable that there is no LAE except for the RG in any of the notable dense group cores of HAEs in spite of the 4σ overdensity in LAEs in this protocluster as a whole on a ∼10 co-Mpc scale. To evaluate the deficiency of LAEs in the local overdensities, this work defines a density parameter, the mean projected distance $\langle a \rangle_{\rm Nth} = 2 \times (\pi \Sigma_{\rm Nth})^{-0.5}$ where $\Sigma_{\rm Nth}$ $(= {\rm N}/(\pi r_{\rm Nth}^2))$ is the number density of HAEs within the radius $r_{\rm Nth}$ which is the distance to the (N−1)th neighbours from each HAE. We use N=5. We stress that this density parameter maintains a relative consistency even if we choose different N values.

The median value and the scatter of the mean projected distance ($\langle a \rangle_{\rm 5th}$) is 214^{+140}_{-88} ph-kpc. We investigate the significance of the LAE deficiency in the dense groups by dividing the HAE samples into high density and low density sub-samples separated at this median value. The fractions of LAEs among HAEs are 21 ± 11 % in the lower densities and only 2 ± 4 % excluding the RG (or 4 ± 5 % with the RG) in the high-density regions, respectively. Fig. 3 represents the cumulative distributions of $\langle a \rangle_{\rm 5th}$ (upper panel) and stellar mass (lower panel) for the HAEs and the HAEs with Lyα emission detections. Stellar masses of the HAE samples are provided by Hayashi et al. (2016). In the upper panel, the possibility that "HAEs" and "HAEs+LAEs" are drawn from the same distribution is only 2 % according to the Kolmogorov-Smirnov test, suggesting that Lyα photons are more depleted in high-density regions. This trend is still statistically significant (p=0.04) even if we use the mass-control samples where we limit the galaxies only with the stellar masses lower than 10^{10} $M_\odot$. Even if we go further down in stellar masses, where such a statistical test would become no longer significant, the LAE deficiency at $\langle a \rangle_{\rm 5th} < 300$ ph-

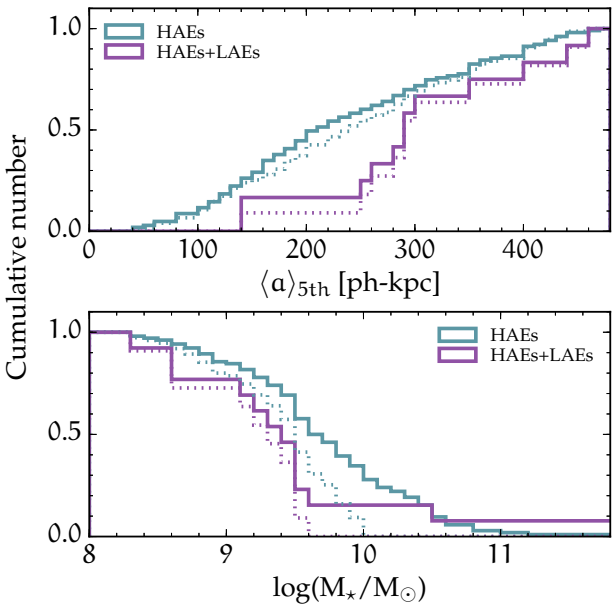

Figure 3. Normalised cumulative distributions of (a: upper) the mean distances and (b: lower) stellar mass. The blue and purple solid lines indicate the entire HAE samples and HAEs with significant Lyα emission, respectively. The dotted lines show the mass-control sample with $M_\star < 1E10^{10}$ $M_\odot$.

kpc would still remain. In fact, we do not see a significant difference in stellar mass distributions between the HAEs and those with Lyα emission lines; p-value is 0.07 for the entire sample and is 0.18 for the mass-control sample, respectively. Such an insignificant or small difference in stellar mass distributions between LAEs and non-LAEs is consistent with the recent studies (Hagen et al. 2016; Hathi et al. 2016). We stress that we here employ only the LAEs whose Hα emission lines are detected (as HAEs) by the independent narrowband imaging at NIR. Therefore, these comparisons are free from the contaminations in our LAE samples which could be a problem only for the LAE-only samples.

4 DISCUSSION AND SUMMARY

Our dual Lyα and Hα line survey of a protocluster at $z = 2.5$ presented has provided us with the first critical insight into the environmental dependence of the Lyα strength as compared to Hα. The broad agreement in the spatial distributions between LAEs and HAEs on a large scale ($\gtrsim 10$ co-moving Mpc) indicates that Lyα line would be a good tracer of LSSs in the high-z Universe. On a smaller scale, however, we see that LAEs, except for the RG, completely avoid the protocluster's dense cores, which are traced by the overdensities of HAEs. This means that the LAE surveys of protoclusters would inevitably miss the particularly dense regions of protoclusters which are likely to be the most interesting and critical environments where we expect to see any early environmental effects as the progenitors of present-day rich cluster cores. In other words, we are not really able to study environmental effects with the LAEs alone as they can trace only the outskirts of protocluster cores or even larger-scale structures around them. In order to search for truly dense structures at $z > 2.6$ where Hα is no longer available, the James Webb Space Telescope (Gardner et al. 2006) will be very powerful as it probes the rest-frame optical regime where many nebular emission lines other than Lyα are located. It should be noted, however, that bright Lyα blobs can be also used as a tracer of the central galaxies in massive haloes as suggested by the past studies (e.g. Steidel et al. 2000; Matsuda et al. 2011).

We measure the escape fraction of Lyα photons by comparing the Lyα and Hα fluxes. This can quantify the deficiency of LAEs in the protocluster's dense cores and thus provide insight into its physical origins. Unfortunately, the current datasets are not deep enough to estimate the escape fraction of Lyα photons for individual HAEs, and thus we conduct the stacking analysis and derive Hα and Lyα luminosities with high precision. The entire HAE samples are divided into two sub-samples by their local 2-D densities at the median value of the fifth mean distance (214 ph-kpc). The narrowband images are then combined with the IMCOMBINE task by median on IRAF[2]. We derive Hα and Lyα fluxes in the same way we measure the individual HAEs and LAEs in Hayashi et al. (2016); Shimakawa et al. (2016). Photometric errors are estimated with a similar approach taken by Skelton et al. (2014) where the 1-sigma Gaussian noise in background counts is measured as a function of variable aperture size. Our error measurements are thus performed independently of the SExtractor photometries since the SExtractor does not consider the pixel-to-pixel correlation and thus underestimates the errors especially for photometries with large aperture sizes. More details of the stacking method and the measurements of fluxes and errors will be presented in a forthcoming full paper (Shimakawa et al. 2017). We assume a 10 % flux contamination from [NII] line to the narrowband flux for Hα, and 0.7 mag of dust extinction in Hα flux. The Lyα escape fraction is given by $f_{\rm esc}^{\rm Ly\alpha} = (f_{\rm Ly\alpha,obs})/(8.7 f_{\rm H\alpha,int})$ where 8.7 is the ratio of Lyα to Hα under the assumption of case B recombination (Brocklehurst 1971). This work estimates Lyα and Hα fluxes with various aperture radii from 6 to 30 ph-kpc taking into account the fact that most of the star-forming galaxies show diffuse Lyα components (Östlin et al. 2009; Steidel et al. 2011; Hayes et al. 2013).

We compare the measured Lyα photon escape fractions between the HAEs in high-density regions and those in lower-density regions. Both composite line images seem to have diffuse Lyα profiles since the escape fraction increases with aperture radius, although photometric errors are quite large. In addition, we see Lyα absorption features within the small aperture radii, which are consistent with the individual detection of Lyα absorption in massive HAEs in the random field (Shimakawa et al. 2016). Most importantly, we find systematically lower Lyα photon escape fractions for the denser regions. This means that the Lyα emission lines are systematically more depleted in denser regions than in lower-density regions in the protocluster (Fig. 4). However, we should note that the Lyα photon escape fraction is considered to depend on various physical properties such as dust, SFR, and metallicity (Hayes et al. 2010; Matthee et al. 2016) that could depend on the environment. The discrepancy between the two composite HAEs may

[2] http://iraf.noao.edu

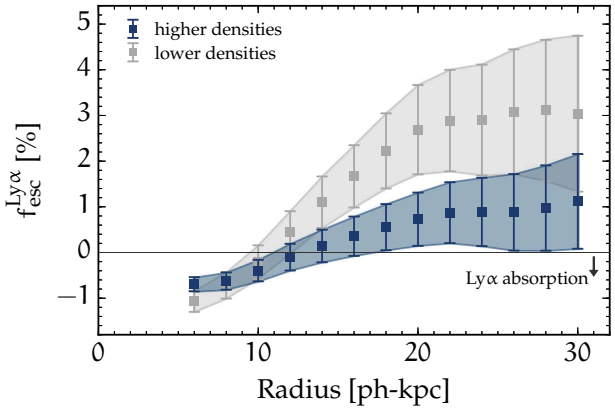

Figure 4. Based on the stacking analysis, the Lyα photon escape fractions ($f_{esc}^{Ly\alpha}$) of the composite HAEs are shown as a function of photometric aperture radius within which we integrate line fluxes. Here, the HAE samples are split into two sub-samples at the median value of the mean projected distance ($\langle a \rangle_{5th} = 214$ ph-kpc). The composite HAEs in the higher/lower density regions are presented by blue/grey zones, respectively. The errorbars represent the photometric errors in Lyα and Hα line fluxes. The negative $f_{esc}^{Ly\alpha}$ values mean that Lyα is seen as an absorption line.

also contain such secondary factors on top of the environment. Moreover, the narrowband technique cannot resolve the detailed spectral features around the Lyα line. Thus our measurements may underestimate the escape fraction due to absorption by foreground circumgalactic/intergalactic medium (CGM/IGM) (Hayes & Östlin 2006) and/or blue-shifted dense outflowing gas (Reddy et al. 2016).

In summary, we find that LAEs are missing in the dense HAE cores. We also find that Lyα photon escape fractions in the composite HAEs in the denser regions are lower than those in lower-density regions. In the general field, it is expected that LAEs have less dust and lower HI covering fractions (Shibuya et al. 2014; Reddy et al. 2016) and therefore Lyα photons can relatively easily escape from the galaxies. However, in the protocluster core, we have extra surrounding gas and dust components trapped in the group/cluster scale haloes, which may prevent the Lyα photons from escaping from the systems. Such abundant group-scale HI gas may be supplied from the surrounding regions, for example, by cold streams (Dekel et al. 2009a,b). Moreover, since the mean projected distance of HAEs is much smaller ($\lesssim 200$ ph-kpc) in higher-density regions than in the lower-density regions, Lyα photons emitted from a HAE have a higher chance of penetrating CGM associated to other member galaxy(ies) in the foreground located along the line of sight, and thus they may be more depleted. Otherwise, most of the individual galaxies in the dense cores could originally have lower Lyα photon escape fractions due for example to higher dust extinction by a certain environmental effect (Koyama et al. 2013). The current datasets are clearly insufficient to conclusively choose the most plausible explanation (further discussion will be described in Shimakawa et al. 2017). A deep, rest-frame FUV spectroscopy of the protocluster galaxies with LRIS and/or KCWI on Keck telescope will be helpful for us to constrain the physical origins of the Lyα depletion effect and to resolve the interplay between protocluster galaxies and CGM/IGM.

ACKNOWLEDGEMENTS

The data are collected at the Subaru Telescope, which is operated by the National Astronomical Observatory of Japan. This work is subsidized by JSPS KAKENHI Grant Number 15J04923. This work was also partially supported by the Research Fund for Students (2013) of the Department of Astronomical Science, SOKENDAI. We thank the anonymous referee for useful comments. R.S. and T.S. acknowledge the support from the Japan Society for the Promotion of Science (JSPS) through JSPS research fellowships for young scientists. T.K. acknowledges KAKENHI No. 21340045.

REFERENCES

Bertin E., Arnouts S., 1996, A&AS, 117, 393
Brocklehurst M., 1971, MNRAS, 153, 471
Cappellari M., et al., 2011, MNRAS, 416, 1680
Chabrier G., 2003, PASP, 115, 763
Cole S., Lacey C. G., Baugh C. M., Frenk C. S., 2000, MNRAS, 319, 168
Dekel A., et al., 2009a, Nature, 457, 451
Dekel A., Sari R., Ceverino D., 2009b, ApJ, 703, 785
Dressler A., 1980, ApJ, 236, 351
Fitzpatrick E. L., 1999, PASP, 111, 63
Gardner J. P., et al., 2006, Space Sci. Rev., 123, 485
Hagen A., et al., 2016, ApJ, 817, 79
Hathi N. P., et al., 2016, A&A, 588, A26
Hayashi M., Kodama T., Tadaki K.-i., Koyama Y., Tanaka I., 2012, ApJ, 757, 15
Hayashi M., Kodama T., Tanaka I., Shimakawa R., Koyama Y., Tadaki K.-i., Suzuki T. L., Yamamoto M., 2016, ApJ, 826, L28
Hayes M., Östlin G., 2006, A&A, 460, 681
Hayes M., et al., 2010, Nature, 464, 562
Hayes M., et al., 2013, ApJ, 765, L27
Kajisawa M., Kodama T., Tanaka I., Yamada T., Bower R., 2006, MNRAS, 371, 577
Kodama T., Tanaka I., Kajisawa M., Kurk J., Venemans B., De Breuck C., Vernet J., Lidman C., 2007, MNRAS, 377, 1717
Koyama Y., et al., 2013, MNRAS, 434, 423
Matsuda Y., et al., 2011, MNRAS, 410, L13
Matthee J., Sobral D., Oteo I., Best P., Smail I., Röttgering H., Paulino-Afonso A., 2016, MNRAS, 458, 449
Miyazaki S., et al., 2002, PASJ, 54, 833
Oke J. B., Gunn J. E., 1983, ApJ, 266, 713
Östlin G., Hayes M., Kunth D., Mas-Hesse J. M., Leitherer C., Petrosian A., Atek H., 2009, AJ, 138, 923
Ouchi M., et al., 2003, ApJ, 582, 60
Ouchi M., et al., 2004, ApJ, 611, 660
Reddy N. A., Steidel C. C., Pettini M., Bogosavljević M., Shapley A. E., 2016, ApJ, 828, 108
Schlafly E. F., Finkbeiner D. P., 2011, ApJ, 737, 103
Schlegel D. J., Finkbeiner D. P., Davis M., 1998, ApJ, 500, 525
Shapley A. E., Steidel C. C., Pettini M., Adelberger K. L., 2003, ApJ, 588, 65
Shibuya T., et al., 2014, ApJ, 788, 74
Shimakawa R., Kodama T., Tadaki K.-i., Tanaka I., Hayashi M., Koyama Y., 2014, MNRAS, 441, L1
Shimakawa R., et al., 2015, MNRAS, 451, 1284
Shimakawa R., et al., 2016, preprint, (arXiv:1607.08005)
Shimakawa R., et al., 2017, in preparation
Skelton R. E., et al., 2014, ApJS, 214, 24
Sobral D., et al., 2016, preprint, (arXiv:1609.05897)
Steidel C. C., Adelberger K. L., Shapley A. E., Pettini M., Dickinson M., Giavalisco M., 2000, ApJ, 532, 170

Steidel C. C., Bogosavljević M., Shapley A. E., Kollmeier J. A., Reddy N. A., Erb D. K., Pettini M., 2011, ApJ, 736, 160
Sunyaev R. A., Zeldovich Y. B., 1972, A&A, 20, 189
Venemans B. P., et al., 2007, A&A, 461, 823
White S. D. M., Frenk C. S., 1991, ApJ, 379, 52
Yagi M., Kashikawa N., Sekiguchi M., Doi M., Yasuda N., Shimasaku K., Okamura S., 2002, AJ, 123, 66
van Dokkum P. G., et al., 2011, ApJ, 743, L15

This paper has been typeset from a TEX/LATEX file prepared by the author.